Paper 6.1

Installation Effects on Venturi Tubes of Convergent Angle 10.5º

Michael Reader-Harris, Ronnie Rushworth and Jeff Gibson
NEL

INSTALLATION EFFECTS ON VENTURI TUBES OF CONVERGENT ANGLE 10.5°

Dr Michael Reader-Harris, NEL
Mr Ronnie Rushworth, NEL
Dr Jeff Gibson, NEL

1   INTRODUCTION

With gas production scenarios now frequently involving multiple gas fields, it is important that confidence in the measurements made by wet gas meters is increased as this will ultimately help to increase the viability of marginal gas fields. There is an increasing desire to use Venturi tubes for wet gas measurement, but to ensure accuracy in wet gas it is necessary to understand their behaviour in dry gas first.   It was generally assumed until about eight years ago that the discharge coefficient at high Reynolds number in high-pressure gas would be constant and approximately equal to that obtained in water at Reynolds numbers greater than 2×10^5. However, work carried out at NEL and reported by Jamieson et al[1], data reported by van Weers et al[2], and subsequent work at NEL[3-7] have shown that the performance of Venturi tubes in gas is very different from that in water. Some discharge coefficients in gas are greater than would have been expected by 3 per cent or even more.

One factor which has an effect on how a Venturi tube performs is its internal shape. Work at NEL[8] showed that, of the designs evaluated, the optimum design was one with a convergent angle of 10.5° and sharp corners.

It was therefore necessary to investigate installation requirements for a Venturi tube with a convergent angle of 10.5° and sharp corners. It was decided to determine the influence on the discharge coefficient of two fittings located at a number of distances upstream of each of three Venturi tubes of this design.

CFD has proved to be useful in the analysis of gas and wet gas flows through conventional Venturi tubes. CFD was used to compute the effect of a single bend on Venturi tubes with convergent angles of 10.5° and 21°.

2   DESCRIPTION OF THE VENTURI TUBES

Three Venturi tubes of convergent angle 10.5° and sharp corners of diameter 100 mm with diameter ratios, β, of 0.4, 0.6 and 0.75 were used. The Venturi tubes had been manufactured to drawings with tight tolerances designed to ensure that where possible the results were not affected by uncontrolled variables. They were made of stainless steel and were designed not only to meet the requirements of ISO 5167-1:1991[9] but to follow its recommendations. The Standard recommends the use of a divergent angle between 7° and 8°: 7½° was specified.

So that the results would not be corrupted by the introduction of steps at joins in the pipework, machined pipework, much of which had been honed, was used close to the Venturi tubes. This pipe had previously been manufactured by boring out Schedule 80 pipe to the bore of a Schedule 40 pipe. For the baseline test there were lengths totalling 42*D* of machined pipe upstream of the Venturi tubes and a downstream machined length of 8*D*, where *D* is the diameter of the entrance cylinder. The lengths of pipe and the Venturi tubes were dowelled to ensure concentricity; O rings were used to ensure that there would not be recesses or protruding gaskets. The distance from the upstream pressure tappings to the first upstream flange was 1.1*D.*

An additional 21*D* length had been manufactured by welding a 19*D* length of Schedule 40 pipe to a 2*D* length of pipe machined to the bore of the other pipes, smoothing off any step at the weld. This length of pipe was installed with the machined length adjacent to the machined pipe already described, so that there was 45*D* of machined pipework, whose bore matched that of the Venturi tube very accurately, immediately upstream of the upstream tappings of the Venturi tube. In total

there was 64D of pipe of the same schedule with no recesses, protruding gaskets or significant steps upstream of the Venturi tube. Upstream of this assembly, there was 18D of pipe of the same nominal diameter preceded by a flow conditioner. Downstream of the machined pipe already described there was at least 7D of pipe of the same nominal diameter.

For the tests of installation effects, first a single 90° bend and then two close-coupled 90° bends in perpendicular planes were used. The first installation provides an asymmetric flow, the second a swirling flow with some asymmetry. The bends were of radius 1.5D and had a parallel section of length 0.8D; so between the curved portions of the two closely coupled bends was a straight length of 1.6D. Upstream of the single bend there was a length of 20D of Schedule 40 pipe preceded by 25D of pipe of the same nominal diameter preceded by a flow conditioner.

3   MEASUREMENTS OF THE EFFECT OF UPSTREAM BENDS

The data were collected in water in the large water flow facility using water/air and water/mercury manometers. For each Venturi tube the data in water lay on a straight line as a function of pipe Reynolds number, Re_D, and with a small scatter, provided that Re_D was above a critical value. In subsequent analysis only data for which $Re_D/10^6$ was greater than 0.165, 0.3 or 0.5 for β = 0.4, 0.6 and 0.75 respectively were included. Distances are measured from the end of the curved portion of the bend closest to the Venturi tube to the upstream pressure tappings of the Venturi tube. To illustrate the method of analysis, the baseline data for the Venturi tube of β = 0.6 and the data collected with a single bend 2.7D upstream of it are shown in Figure 1. Lines have been fitted to both sets of data and are shown. The mean value of $Re_D/10^6$ for the data collected with a single bend 2.7D upstream is 0.472 and is marked on the figure; this value gives the minimum uncertainty for that line. The difference between the fitted line for the installation at this value of $Re_D/10^6$ and the baseline is evaluated and considered to be the shift for this installation. It is marked on Figure 1 (in this case ΔC is negative).
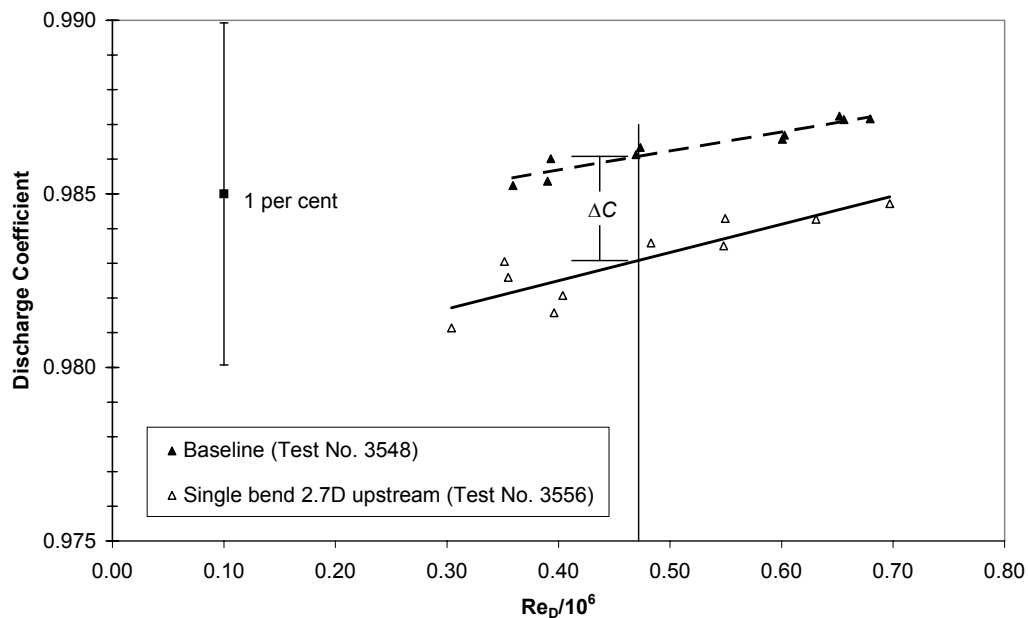

Figure 1 Shift in discharge coefficient with a single bend 2.7D upstream of a Venturi tube of β = 0.6

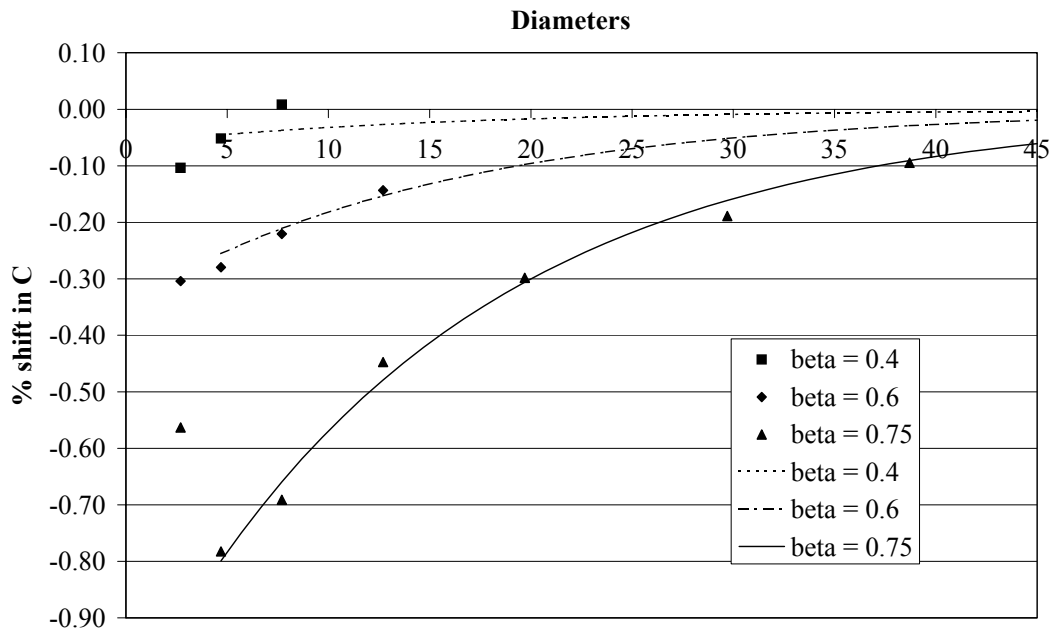The calculated shifts are shown in Figures 2 and 3.

Diameters

Figure 2 Shifts in discharge coefficient downstream of a single bend
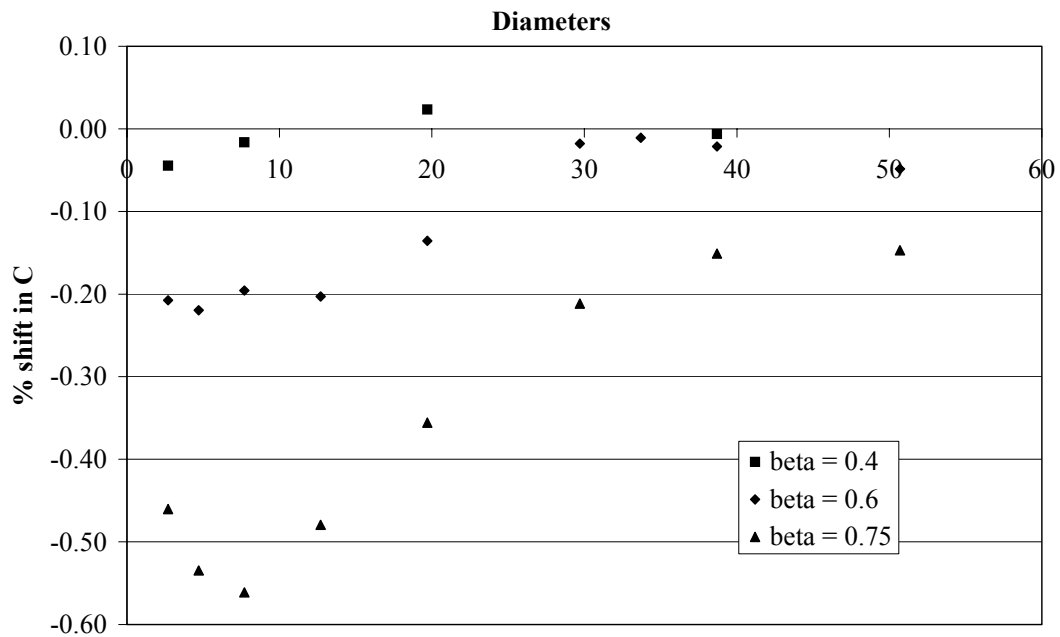
Diameters

Figure 3 Shifts in discharge coefficient downstream of two bends in perpendicular planes

The data on Figure 2 for $x/D \geq 4.7$, where x is the distance between a fitting and the upstream pressure tappings of a Venturi tube, are well fitted by

$$\frac{100 \Delta C}{C} = -2.321 \frac{\beta^4}{1 - \beta^4} e^{-0.064 x/D} .$$

This equation is shown on Figure 2. A similar fit could be obtained to the data shown on Figure 3, but, although quite good agreement with the data would be obtained, it would fail to include some important (if small) features of the data.

If the shifts in discharge coefficient downstream of these two fittings obtained here are compared with those for standard Venturi tubes with convergent angle 21° then the striking feature particularly of the single-bend data is that the data with a 10.5° convergent fall into the expected pattern as a function of β (similar to the pattern for orifice plates as seen for example in Section 6 of Reference 10 and in Zedan and Teyssandier[11]), whereas the data with a 21° convergent do not. Measurements of installation effects on standard 6-inch (150 mm) Venturi tubes (with machined convergent sections and convergent angle 21°) were made at NEL[12]: the weldnecks were of length 50 mm so that the distance between the curved portions of the bends should be small. Those calibrations are in good agreement with the data of Himpe et al[13] (as seen in Figures 8 – 10 later in this paper), particularly for the larger values of β, and those of Reference 14 quoted by Kochen et al[15]. Both Himpe et al and Reference 14 had a pipe diameter of 100 mm. If, as appears to be the case, reducing the angle of the sharp corner at the upstream end of the throat has significant benefits in high-pressure gas[8], then it may improve the pattern of the installation-effect data in the same way.

The required straight lengths upstream of a standard Venturi tube (with a 21° convergent angle) are given in Table 1 of ISO 5167-4:2003[16] and shown in Table 1, and were based on the data in References 12-14. If these lengths were used for Venturi tubes with a 10.5° convergent angle they would be conservative for β = 0.4 and 0.6 but inadequate for β = 0.75, if the aim is that shifts should be less than 0.25 per cent. The straight lengths in Table 1 of ISO 5167-4:2003 are sufficient for Venturi tubes of convergent angle 10.5° for β up to about 0.67. If the required upstream straight lengths for Venturi tubes of convergent angle 10.5° were evaluated on the basis of the data collected in this project and of shifts being less than 0.25 per cent for column A and 0.75 per cent for column B they would be as given in Table 1. If all the data gave shifts less than 0.25 per cent column B was left blank.

Diameter ratio β	21° convergent angle (ISO 5167-4: 2003)				10.5° convergent angle			
	Single 90° Bend		Two or more 90° bends in the same plane or different planes		Single 90° Bend		Two 90° bends in perpendicular planes	
	A	B	A	B	A	B	A	B
0.3	8	3	8	3	3		3	
0.4	8	3	8	3	3		3	
0.5	9	3	10	3	3		3	
0.6	10	3	10	3	6	3	3	
0.7	14	3	18	3	17	3	22	3
0.75	16	8	22	8	24	6	27	3

Table 1 Required straight lengths upstream of Venturi tubes

## 4   COMPUTATIONS OF THE EFFECT OF UPSTREAM BENDS

4.1   Introduction to the Computational Fluid Dynamics work

Computational Fluid Dynamics (CFD) was used to compute the effect of a 1.5*D*-radius single bend on the performance of 4-inch Venturi tubes with β = 0.4, 0.6 and 0.75 in water at a Reynolds number of 350,000 and at various distances from the bend. Two sets of Venturi tubes were analysed: the first had a standard convergent angle of 21°, the second had a non-standard convergent angle of 10.5° for comparison with the experimental data in Section 3.

The effect of the single bend on the Venturi tubes was modelled in two parts, the output from the first being input to the second. The first model, the single-bend model, comprised a 1.5*D*-radius single bend, followed by 50*D* of straight pipe (Figure 4).   The second model consisted of the relevant Venturi tube (Figure 5). Once the single bend model had converged to a solution, the velocity and turbulence parameters were taken from slices through the long pipe section and input to the Venturi tube models at distances of 3, 5, 8, 12 and 20*D* from the

bend. Some additional models were run at distances of 30 and 40D from the bend in order to match available test data.

As the flow through a single bend is symmetrical about the X-Y plane (z = 0), this meant that only half of the domain needed to be modelled, optimising on cell-count (note: the mesh shown on Fig. 4 has been reflected about the z = 0 plane). In addition, the cell count was relaxed in the direction of the flow, with the majority of the cells being concentrated through the bend.   Two meshes were used to model the flow, one finer than the other to investigate the effect of grid dependency on the solution.   The fine mesh (as shown on Fig. 4) employed some 137,000 cell volumes, with 912 cell faces across the plane of the pipe (inset). The coarse mesh employed just over 32,000 cell volumes, with 432 cell faces across the plane of the pipe.
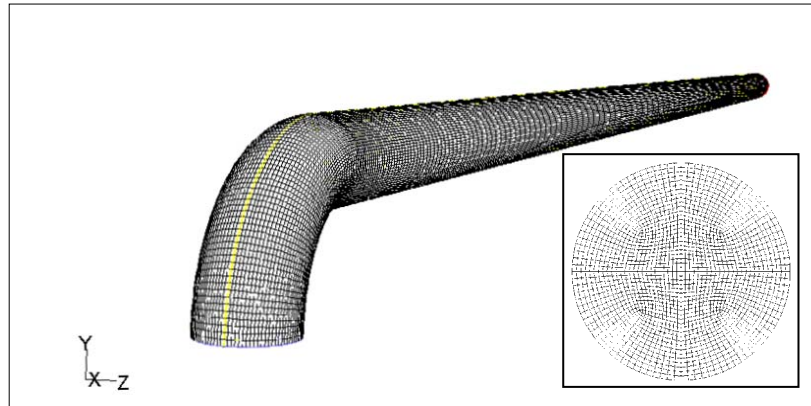
Figure 4 Mesh used to simulate the flow through the single bend (fine grid shown)

The Venturi tube models with fine meshes employed between 138,000 and 158,000 cells in total, depending on β and convergent angle, with the grid in the cross section matching that of the single bend model. Once again, cell bunching was used to concentrate cells in the throat region in order to reduce the number of cells required.   The coarser mesh was only run for β = 0.75, and a convergent angle of 21°, and comprised 61,000 cells in total, with 432 across the plane of the pipe. In both cases, the grid across the plane of the Venturi tubes matched up exactly with the corresponding single bend model to avoid interpolation errors.
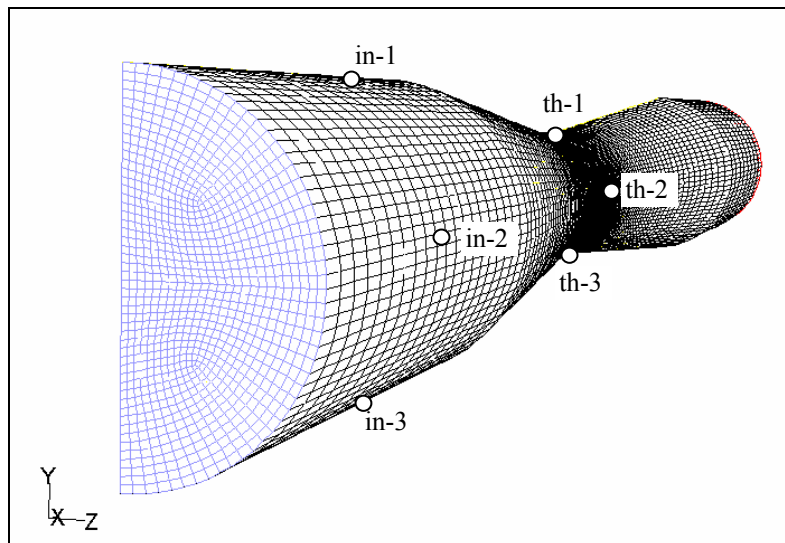
Figure 5 Mesh used to simulate the flow through the β = 0.6 Venturi tube (circles indicate the positions of the taps at the inlet and throat planes respectively)

5

4.2 Method

The effect of the single bend was given by the percentage shift in discharge coefficient, *C*, obtained by comparing the solution run with input from the single bend model with the baseline obtained using a fully developed profile. The fully developed solutions were obtained using separate axisymmetric models - one for each value of β. The effect of the pressure tappings on the shift was assumed to be negligible and the pressure tappings were excluded from the models. The discharge coefficient predicted by the CFD was evaluated using the standard equation for an incompressible flow.

The pressure at the inlet and throat planes was taken to be the arithmetic average of the wall pressures taken at the tapping positions labelled on Figure 5, clockwise from the top as 1-4, with the subscripts 'in' and 'th' referring to the inlet and throat tapping planes respectively. Since the CFD model utilised symmetry about the X-Y plane, the pressure at tapping 2 was doubled to simulate the presence of virtual tap 4

$$p_{av} = \frac{p_1 + p_2 + p_3 + p_4}{4} \equiv \frac{p_1 + 2p_2 + p_3}{4}$$

In the case of the fully developed profile, the flow entering the Venturi tube was axisymmetric and, thus, $p_1 = p_2 = p_3 = p_4$.

4.3 Models used and initial results

The CFD software used was Fluent v6.1[17], with Gambit v2.0 used to mesh the geometry. The models were solved using both the standard k-ε (ske) and the more complicated Reynolds Stress Model (RSM) for turbulence, with the second order interpolation scheme for velocity and turbulence. There was little difference in the results of the models, with the k-ε model appearing to be in better agreement with the test data (see later). As the RSM model generally requires finer grids than the k-ε model to get a grid-independent solution, no particular benefit could be seen in using this model further in this study. The pipe walls were defined as smooth for all computations, with the standard wall function model being used to compute near-wall regions.

Figure 6 illustrates the effect the grid has on the CFD results for the β = 0.75 Venturi tube with 21° convergent angle, as compared with the NEL test data. It is clear that, although the trend is similar up to x/D = 5, further from the bend the coarse-grid solution diverges from the fine-grid solution, lying above it by between 0.3% and 0.4%. The finer grid solution is clearly in better agreement with the test data than the coarse grid solution, although the difference between the two is moderately small.
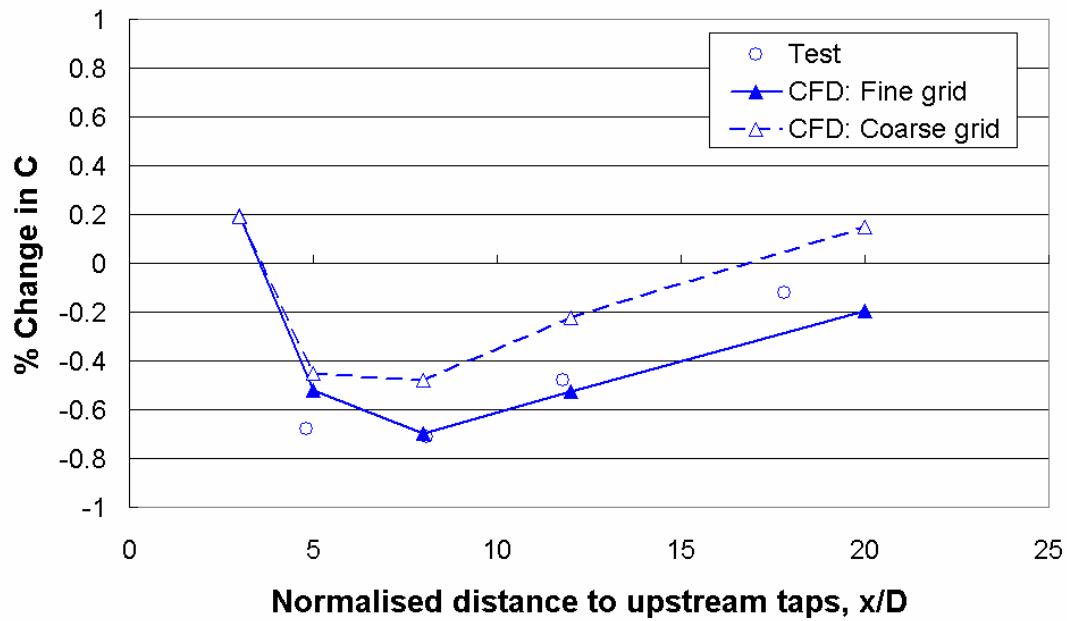
Figure 6 Effect of grid on CFD results for β = 0.75 Venturi tube using the standard k-ε turbulence model (coarse = 61,000 cells, fine = 138,000 cells)

Figure 7 details the results from the β = 0.75 Venturi tube with 21° convergent angle computed using the two turbulence models, as compared with the NEL test data. Although the trends are similar, the standard k-ε model describes the trend in error better with distance from the bend. The RSM model is also more expensive to run in terms of solution time than the standard k-ε model. Therefore, the remainder of the modelling was carried out exclusively using the standard k-ε model.
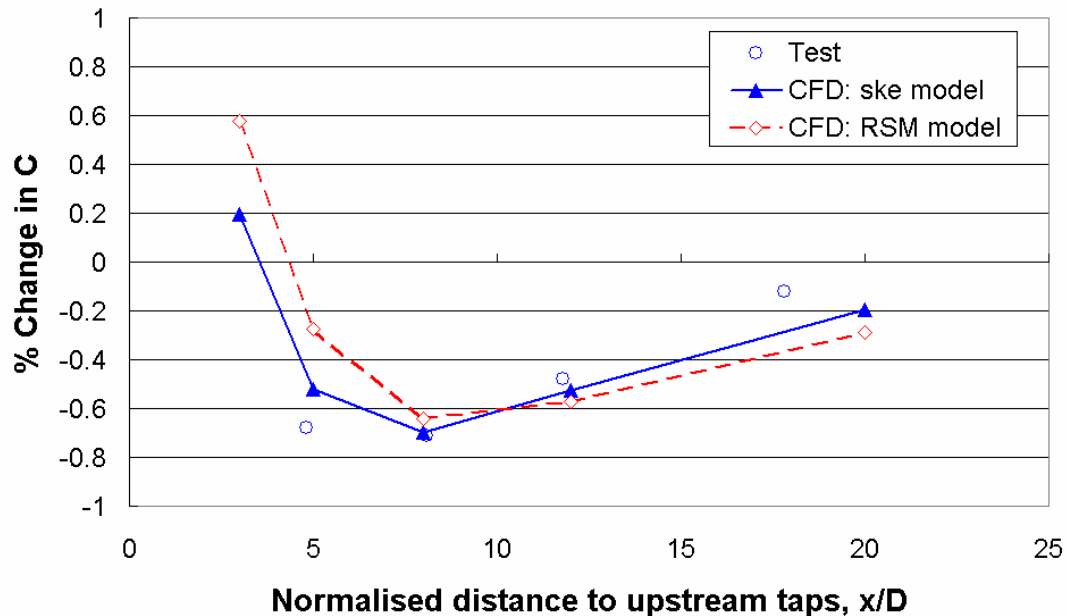
Figure 7 Comparison of CFD with test data for the β = 0.75 Venturi tube using two turbulence models (all computations performed using the fine grid)

4.4 Results from standard Venturi tubes with 21° convergent angle

Figures 8 - 10 detail the CFD results of the standard Venturi tubes with 21° convergent sections, as compared with the test data. The data sets labelled "NEL" refer to the tests undertaken on 6-inch Venturi tubes in water over a range of Reynolds numbers around approximately 3×10^5 for $\beta = 0.4$, 4×10^5 for $\beta = 0.6$, and 6×10^5 for $\beta = 0.75$ and presented for the first time in Reference 12, whilst data labelled "Himpe" refer to the tests undertaken by Himpe et al[13] who tested 4-inch Venturi tubes on water at a Reynolds number of 3.7×10^5.

The results clearly show that the CFD is capable of predicting the correct trend in installation error, both with distance from the bend and with β. At $5D$ downstream of the bend and further, the agreement is within 0.1% of the test data for $\beta = 0.6$ and 0.75. For $\beta = 0.4$ there is a 0.2% shift between the NEL and Himpe test data: the CFD appears to agree quite well with the NEL data.

There is a similar pattern to all of the data sets: as the distance between a Venturi tube and the bend increases from zero the error becomes increasingly negative, until the distance from the bend reaches about 4-8D, after which it then becomes less negative. For the Himpe data, the turning point would appear to occur at $4D$ for all β, whilst the CFD predicts it will occur at about 8D. As the NEL test data do not extend below $5D$, it is more difficult to discern where the turning point actually occurs in this case.

Earlier data collected by Pardoe[18] were very different from the data of References 12-14. Pardoe obtained positive shifts in C downstream of a single bend and stated that 6D was sufficient downstream of a single bend even for $\beta = 0.8$, whereas downstream of two bends in perpendicular planes even 30D was not sufficient (at least for $\beta > 0.55$). Although an explanation for the difference between Pardoe's data and subsequent data is still required the CFD collected here agrees with the data of References 12-14.
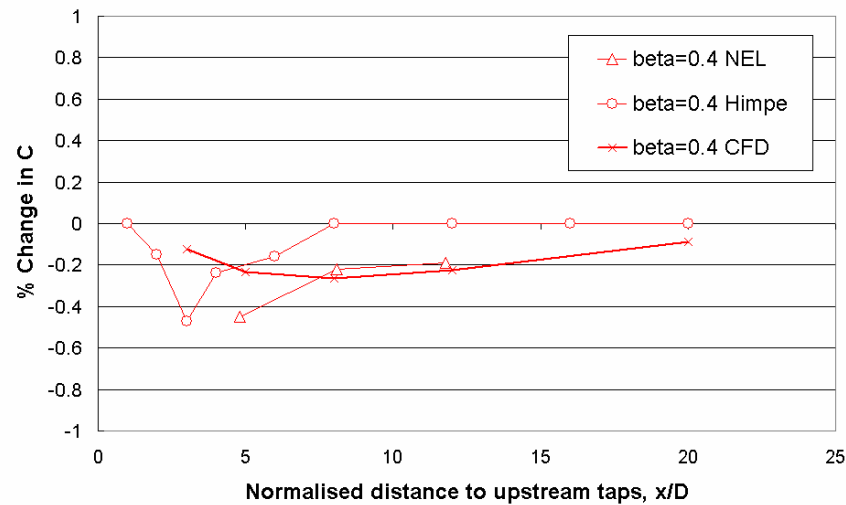

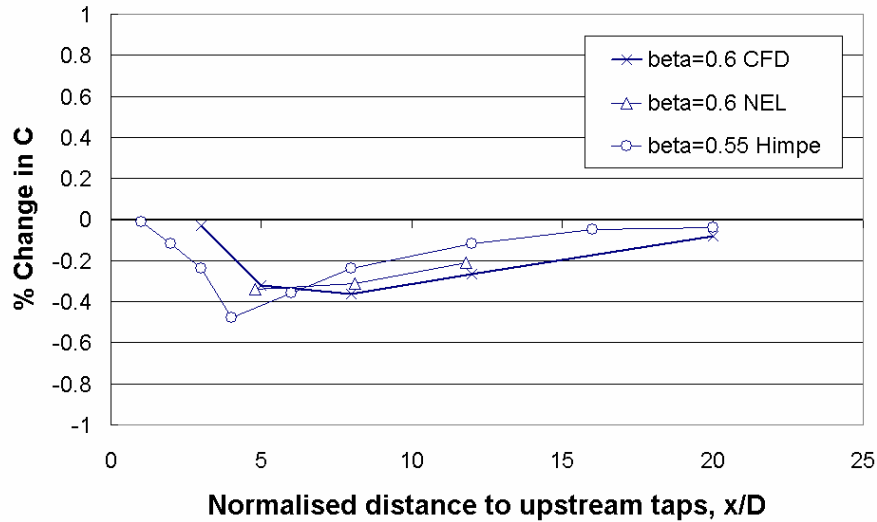**Figure 8 Comparison of CFD results with test data for $\beta = 0.4$ standard Venturi tube**

Figure 9 Comparison of CFD results with test data for β = 0.6 standard Venturi tube
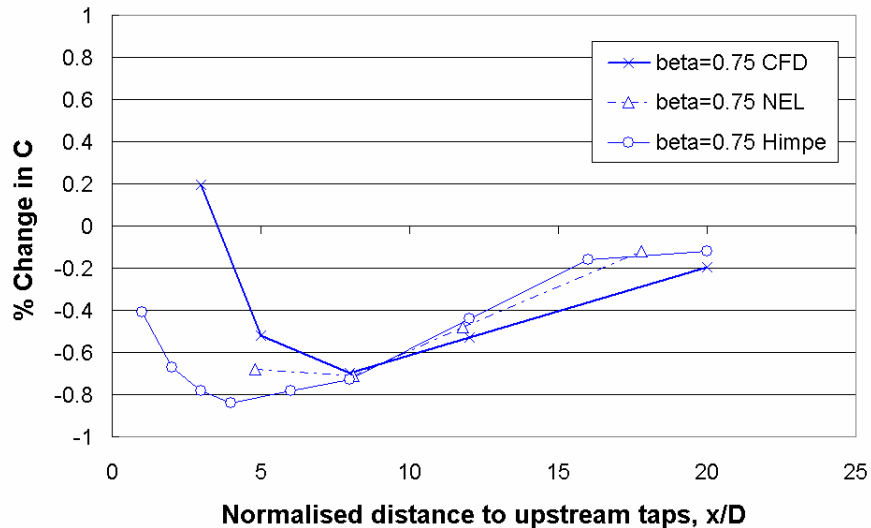

Figure 10 Comparison of CFD results with test data for β = 0.75 standard Venturi tube

4.5   Results from Venturi tubes with 10.5° convergent angle

Figures 11 - 13 detail the CFD results compared with the NEL test results for the Venturi tubes with 10.5° convergent angles. There are clearly differences in the experimental and, to a lesser extent, the CFD results when comparing 10.5° with 21°.   In the case of the β = 0.75 Venturi tubes, the 10.5° data follow the 21° data for the points at 3, 8 and 12D, but appear to diverge beyond this point, lying slightly below the 21° curve.   The 10.5° CFD results follow a similar trend to the 21° case, but there is a cross over point at about 6.5D, resulting in a 0.2% offset between the 10.5° and 21° results. The biggest difference between the two is evident at 3D.

For the β = 0.4 and 0.6 Venturi tubes the 10.5° data lie slightly above those of 21°, as opposed to below them, as in the β = 0.75 case.   The CFD also picks up this effect.

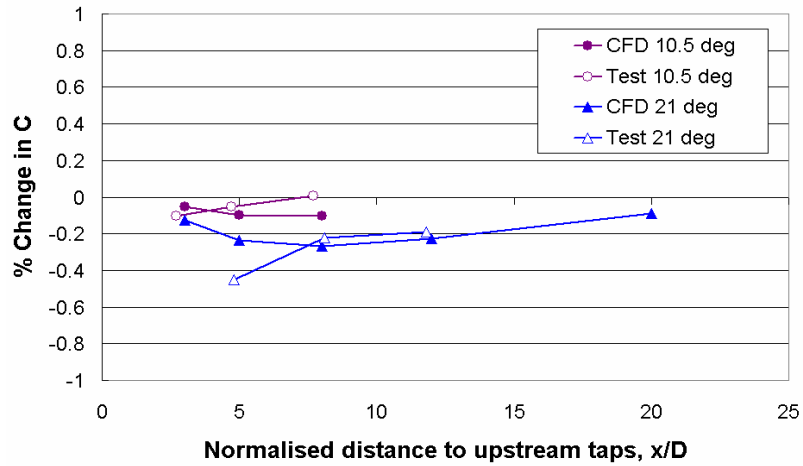The level of agreement between CFD and experiment is very good.

Figure 11 Comparison of CFD with test results for Venturi tubes with 21° and 10.5° convergent angles for β = 0.4.
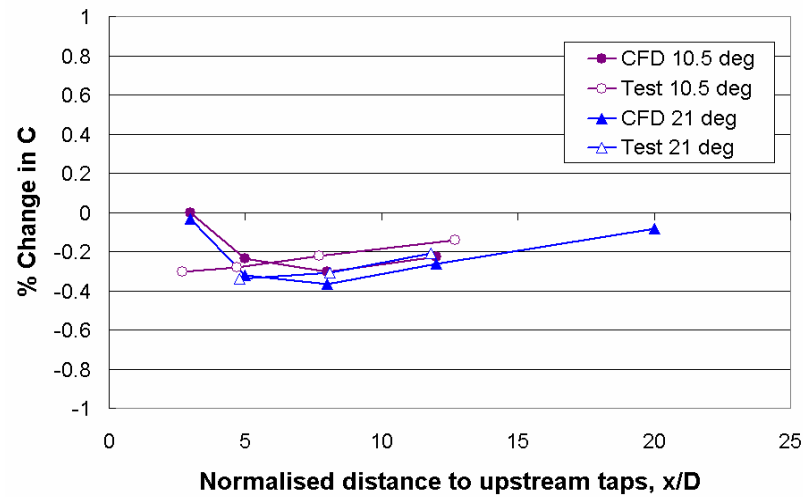

Figure 12 Comparison of CFD with test results for Venturi tubes with 21° and 10.5° convergent angles for β = 0.6.
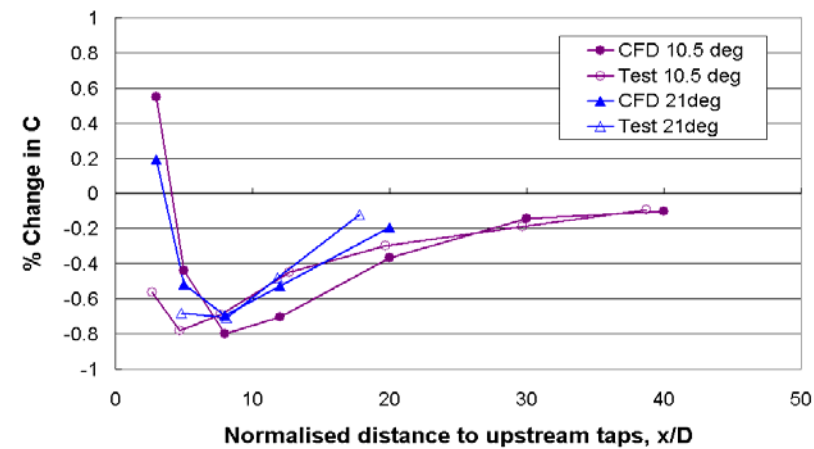

Figure 13 Comparison of CFD with test results for Venturi tubes with 21° and 10.5° convergent angles for β = 0.75.

10

5   CONCLUSIONS

Previous work had shown the benefits of using a Venturi tube with a convergent angle of 10.5° with sharp corners. Here the effect of a single bend and of two bends in perpendicular planes upstream of Venturi tubes of this shape has been evaluated. For small β the required upstream straight lengths for Venturi tubes of convergent angle 10.5° are smaller than those for a standard Venturi tube; for large β they are larger than those for a standard Venturi tube. The straight lengths in Table 1 of ISO 5167-4:2003 are sufficient for Venturi tubes of convergent angle 10.5° for β up to about 0.67.

The effect of upstream installation was also computed using CFD, and very good agreement with experiment was obtained.

The most interesting feature of the data obtained with a convergent angle of 10.5° is that they fall into the expected pattern as a function of diameter ratio, whereas the equivalent data obtained with standard Venturi tubes do not. Reducing the angle of the sharp corner upstream of the throat appears to give more consistent performance in terms of installation effects just as it does at high Reynolds numbers.

ACKNOWLEDGEMENTS

NOTATION

C	Discharge coefficient	-
ΔC	Shift in discharge coefficient	-
D	Diameter of entrance cylinder	m
p	Absolute static pressure	Pa
Q	Volumetric flowrate	m^3/s
Re_D	Pipe Reynolds number $\left(= \dfrac{4Q}{\pi D \nu} \right)$	-
x	Distance between a fitting and the upstream tappings of a Venturi tube	m
β	Diameter ratio (= d/D)	-
ν	Kinematic viscosity	m^2/s

REFERENCES

1   JAMIESON, A. W., JOHNSON, P. A., SPEARMAN, E. P., AND SATTARY, J. A. Unpredicted Behaviour of Venturi Flowmeter in Gas at High Reynolds Numbers. In Proc. of 14th North Sea Flow Measurement Workshop, Peebles, Scotland, paper 5, 1996.

2   VAN WEERS, T., VAN DER BEEK, M. P., AND LANDHEER, I. J. C_d - factor of Classical Venturi's: Gaming Technology?   In Proc. of 9th Int. Conf. on Flow Measurement, FLOMEKO, Lund, Sweden, June, pp. 203-207, 1998.

3   READER-HARRIS, M. J., BRUNTON, W. C., GIBSON, J. J., HODGES, D., and NICHOLSON, I. G.   Venturi tube discharge coefficients.   In Proc. of 4th Int. Symposium on Fluid Flow Measurement, Denver, Colorado, June 1999.

4   READER-HARRIS, M. J., BRUNTON, W. C., GIBSON, J. J., and HODGES, D. Discharge coefficients of Venturi tubes with non-standard convergent angles. In Proc. of FLOMEKO 2000, Salvador, Brazil, June 2000.

5   READER-HARRIS, M. J., BRUNTON, W. C., GIBSON, J. J., HODGES, D., and NICHOLSON, I. G.   Discharge coefficients of Venturi tubes in gas: increasing our understanding.   In Proc. of 'Flow Metering for Next Millennium', FCRI, Palghat, India, September 2000.

6   READER-HARRIS, M. J., BARTON, N., BRUNTON, W. C., GIBSON, J. J., HODGES, D., NICHOLSON, I. G., and JOHNSON, P.   The discharge coefficient and through-life performance of Venturi tubes.   In Proc. of 18th North Sea Flow Measurement Workshop, Gleneagles, ppr 5.2, October 2000.   East Kilbride, Glasgow: National Engineering Laboratory.

7   READER-HARRIS, M. J., BRUNTON, W. C., GIBSON, J. J., HODGES, D., and NICHOLSON, I. G.   Discharge coefficients of Venturi tubes with standard and non-standard convergent angles.   *Flow Measurement and Instrumentation*, Vol. 12, pp 135 – 145, 2001.

8   READER-HARRIS, M. J., BRUNTON, W. C., HODGES, D., and NICHOLSON, I. G. Venturi tubes: improved shape.   In Proc. of 20th Int. North Sea Flow Measurement Workshop, St Andrews, Scotland.   East Kilbride, Glasgow: National Engineering Laboratory, October 2002.

9   INTERNATIONAL ORGANIZATION FOR STANDARDIZATION.   Measurement of fluid flow by means of orifice plates, nozzles and Venturi tubes inserted in circular cross-section conduits running full.   ISO 5167-1, Geneva: International Organization for Standardization, 1991.

10   READER-HARRIS, M. J.   The revision of ISO 5167 – an update.   In Proc. of 16th North Sea Flow Measurement Workshop, Gleneagles, ppr 22, October 1998.   East Kilbride, Glasgow: National Engineering Laboratory.

11   ZEDAN, M. F., and TEYSSANDIER, R. G.   The effect of recesses and protrusions on the discharge coefficient of a flange tapped orifice plate.   ASME Winter Annual Meeting December 1984.   Session: FE-1B-Symposium on differential pressure type fluid meters.

12   READER-HARRIS, M. J., BRUNTON, W. C., and SATTARY, J. A. Installation effects on Venturi tubes.   In Proc. of ASME Fluids Engineering Division Summer Meeting, Vancouver, Canada, FEDSM97-3016, June 1997. New York: American Society of Mechanical Engineers, 1997.

13   HIMPE, U., GÖTTE, B., and SCHATZ, M.   Influence of upstream bends on the discharge coefficient of classical Venturi tubes and orifice plates. *Flow Measurement and Instrumentation*, Vol 5, No 3, pp 209-216, 1994.

14   NATIONAL ENGINEERING LABORATORY.   The influence of the proximity of a 90 degree bend upon the performance of a 100 mm Venturimeter of diameter ratio 0.7069. Report VEDE/01 for VDI/VDE. East Kilbride, Glasgow: National Engineering Laboratory, 1985.

15   KOCHEN, G., SMITH, D. J. M., and UMBACH, H. Installation effects on Venturi tube flowmeters. Intech Engineer's Notebook, pp 41-43, October 1989.

16   INTERNATIONAL ORGANIZATION FOR STANDARDIZATION.   Measurement of fluid flow by means of pressure differential devices inserted in circular cross-section conduits running full – Part 4: Venturi tubes.   ISO 5167-4, Geneva: International Organization for Standardization, 2003.

17   FLUENT EUROPE, LTD. Users' Guide version 6.1, 2001.

18   PARDOE, W. S.   The effect of installation on the coefficients of Venturi meters. *Transactions of the ASME,* Vol. 6, pp 337-349, May 1943.